

Anatomy of the Studied Fourth-order Sequence

The studied fourth-order sequence (Sequence 3), which is 68 feet thick at Pinto and 66.5 feet thick at Mt. Union, is located approximately in the middle of the Wills Creek Formation (the interval between 147 and 213 feet at Pinto in Swartz, 1923). Internally, this fourth-order sequence, at both localities, is divisible into four fifth-order sequences. Lithologically, the first two fifth-order sequences of this fourth-order sequence contain the greatest amount of carbonate while the remaining two fifth-order sequences are predominantly shaley. Therefore, this fourth-order sequence exhibits an overall upward-shallowing trend (Appendix A). Excellent bed-to-bed exposures of this complete fourth-order sequence provide an ideal opportunity for studying the stratigraphic response to long and short eccentricity modulation of the precessional signal.

Small-scale Allocycles

Fifth-Order Sequences

Fifth-order sequences are the most prominent and easily recognized cycles within the studied section of the Wills Creek Formation. These sequences, which average five meters in thickness, are characterized by massive carbonate beds at their bases and by green shaley upper portions. Cycles of this scale were first recognized at Mt. Union, Pennsylvania, by Swartz (1955), who commented that the Wills Creek shale is "composed dominantly of cyclic successions of dolomitic limestone, weathering graying brownish yellow and in part, earthy, overlain by thin-bedded calcareous shale that grades upward into mudrock weathering grayish yellowish green; at some horizons the mudrock

is grayish red or red splotched". Lacey (1960) also recognized these cycles at Mt. Union, describing them as having a basal unit composed of either limestone or dolomite overlain by massive greenish claystone. When Lacey (1960) defined the boundaries, he stated that the change from claystone to carbonate was generally gradational. My field observations indicate that the boundaries between cycles are sharp, marking the abrupt superposition of disjunct facies. In his conclusions, Lacey (1960) suggested the cause of these cyclic patterns was a function of sea-level fluctuations with the carbonate units formed when sea-level was highest and the claystone units when sea-level was the lowest. In contrast, I conclude that these are composite cycles caused by the interaction of two orbital mechanisms.

Their correlation, their thickness and their internal sixth-order cycles justify interpretation of these 5-meter cycles as allogenic fifth-order sequences caused by eccentricity-modulated precession. Correlation of these sequences suggests that they were formed by allogenic mechanisms. Calculations of recurrence interval suggest that those cycles described by Swartz (1955) and Lacey (1960) are best explained as fifth-order cycles (100 ky). Chadwick (1994) found the average thickness of the fifth-order sequences in the Tonoloway to be 3.5 meters. An average thickness of this kind of cycle in the study interval is 5 meters. These values, when applied to the total thickness of the Salina Supersequence (390 meters), suggest that the supersequence contains between 78 and 111 cycles. If the Salina Supersequence is approximately 10 Ma in duration, the recurrence interval of these cycles ranges from approximately 90 ky to approximately 128 ky, encompassing the 100 ky period of the short eccentricity cycle. Thus, these prominent cycles are not precessional cycles.

Each fifth-order sequence is recognized by recurrence of specific facies and a consistent pattern of facies change (Figure 20). Internally, each fifth-order sequence is divisible into meter-scale allocycles. These allocycles qualify as PACs because they exhibit a shallowing-upward pattern and are bounded by surfaces of non-deposition. PAC boundaries within a fifth-order sequence generally are marked by smaller-scale changes in facies than those which define the fifth-order sequence boundaries. Sixth-order sequences have a consistent pattern within the fifth-order sequence. The base of the first PAC (fifth-order boundary) is delineated by a marked change to deeper facies. Generally, the second sixth-order sequence contains the most open facies within the fifth-order sequence. The following three PACs shallow upward episodically.

In the study interval the number of PACs in fifth-order sequences ranges from 3 to 5, indicating that some fifth-order sequences are incomplete. Because Wills Creek fifth-order sequences follow the predicted pattern of having their most open facies in the second PAC (Figure 20), I conclude that PACs are missing from the tops of incomplete sequences, probably by non-deposition (hiatus). All four fifth-order sequences are topped by supratidal green or red shale, indicating subaerial exposure. Dampened precessional rises in this part of the sequence may have been insufficient to either flood this exposed surface or to produce a recognizable facies change. Thus, some of the thick PACs in the upper portion of these sequences (Figures 21, 22 and 30) may actually contain the record of two or more precessional rises.

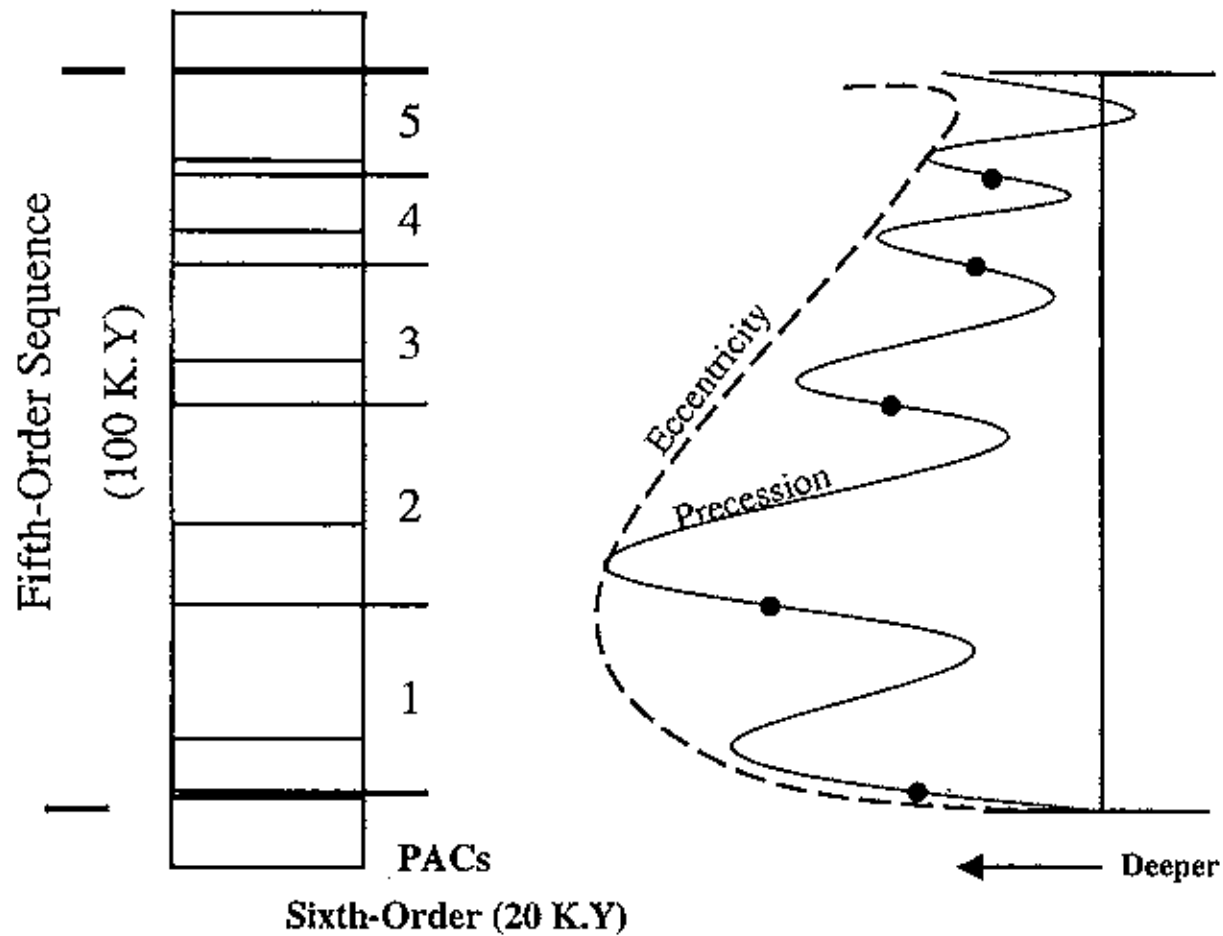


Figure 20. Orbital Variations Relationship to PACs. Ideal schematic fifth-order sequence, with all sixth-order sequences present, and a relative sea-level curve showing eustacy throughout one eccentricity signal. Note that sixth-order boundaries occur at inflection points of sea-level rises. (After Chadwick, 1995)

Sequence A

Fifth-order Sequence A, 19.0 feet thick at Pinto and 14.0 feet thick at Mt. Union is divisible into four PACs at both localities (Figure 21 and 22). At both localities Sequence A (Figure 23 and 27) is initiated and terminated by major facies changes produced by enhanced precessional rises. For example, the base and top of the sequence at Pinto are marked by changes from supratidal green shale to subtidal calcarenite. Sequence A exhibits the typical fifth-order internal facies pattern. An abundance of carbonate and fauna are found in the lower three PACs (between the indicated surfaces, top photo, Figure 23). The deepest facies occur in Cycles A-2 and A-3 (particularly at Pinto) and the thickest interval of shallow (supratidal) facies is in Cycle A-4 at both localities.

An offshore-onshore trend, where Pinto is offshore and Mt. Union is onshore, is evident in Sequence A when comparing the facies of PACs A-1 through A-3 at the two localities. For example, PAC A-1 at both localities contains intertidal carbonate facies at Pinto, and high intertidal to supratidal facies at Mt. Union. In addition, PACs A-2 and A-3 contain subtidal and intertidal skeletal calcarenites at Pinto and are dominated by intertidal and supratidal shale facies Mt. Union (Figures 21, 22 and 26). Greater thickness of subtidal carbonates, diversity and abundance of fauna at Pinto, contrasted with more supratidal (shaley) facies and less fauna at Mt. Union support the relationship of an onshore-offshore trend.

At both localities Sequence A is incomplete, probably because a fifth PAC was not deposited at the top of the sequence. The extensive supratidal facies at the top of

Pinto- Sequence A

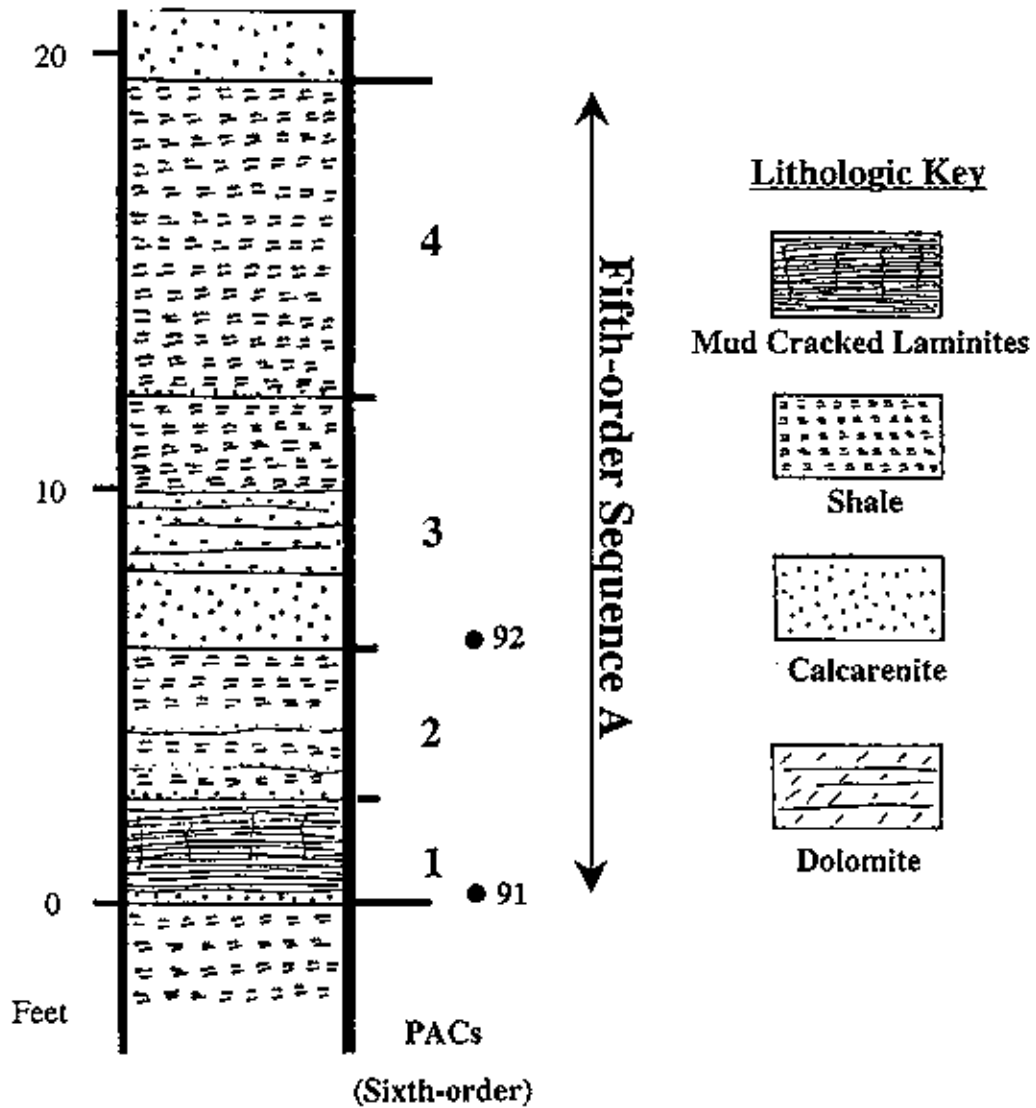


Figure 21. Stratigraphic Column of Sequence A at Pinto. Sequence A is divisible into four PACs, numbered 1 through 4. Numbered black dots indicate sample locations.

Mt. Union-Sequence A

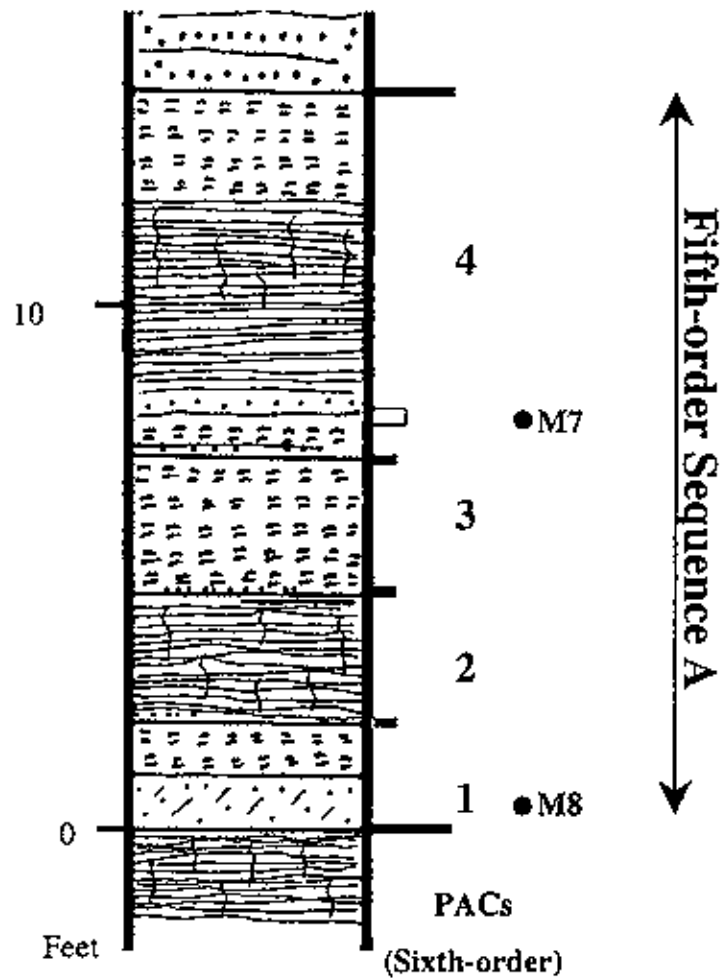


Figure 22. Stratigraphic Column of Sequence A at Mt. Union. Sequence A is divisible into four PACs, numbered 1 through 4. Numbered black dots indicate sample locations.

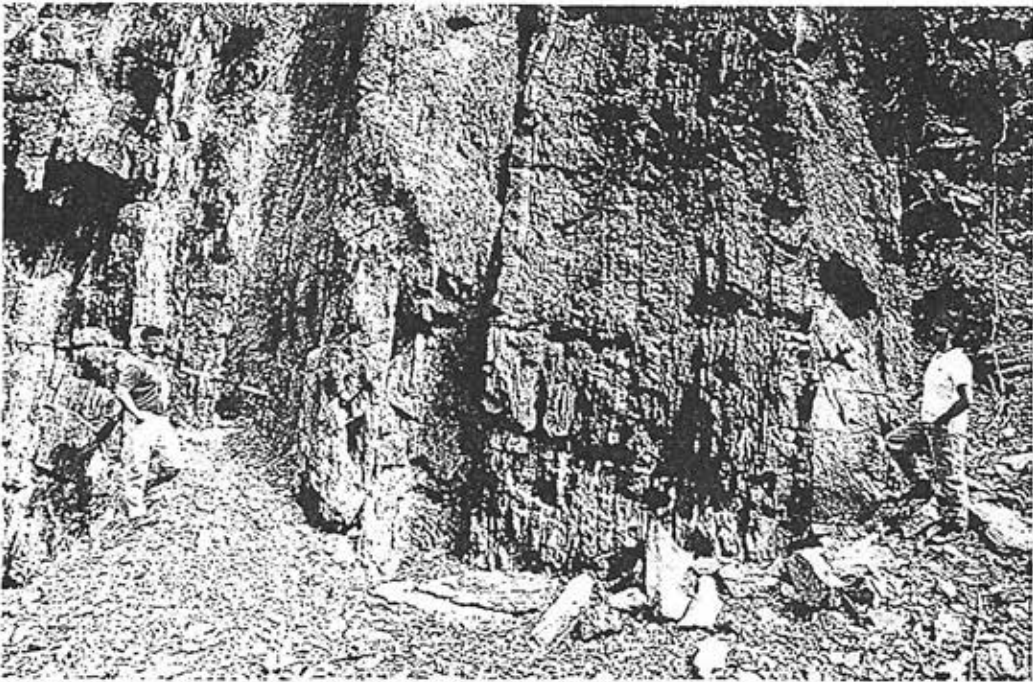


Figure 23. Fifth-order Sequences A and C at Pinto, Maryland. Stratigraphic up is to the left in each photograph. Each sequence is carbonate-rich (resistant beds) at the base and shale-rich at the top. Sequence C (bottom photo) is more shaley than Sequence A (top photo). Sequence B and Cycle A-4 are not exposed at track level.

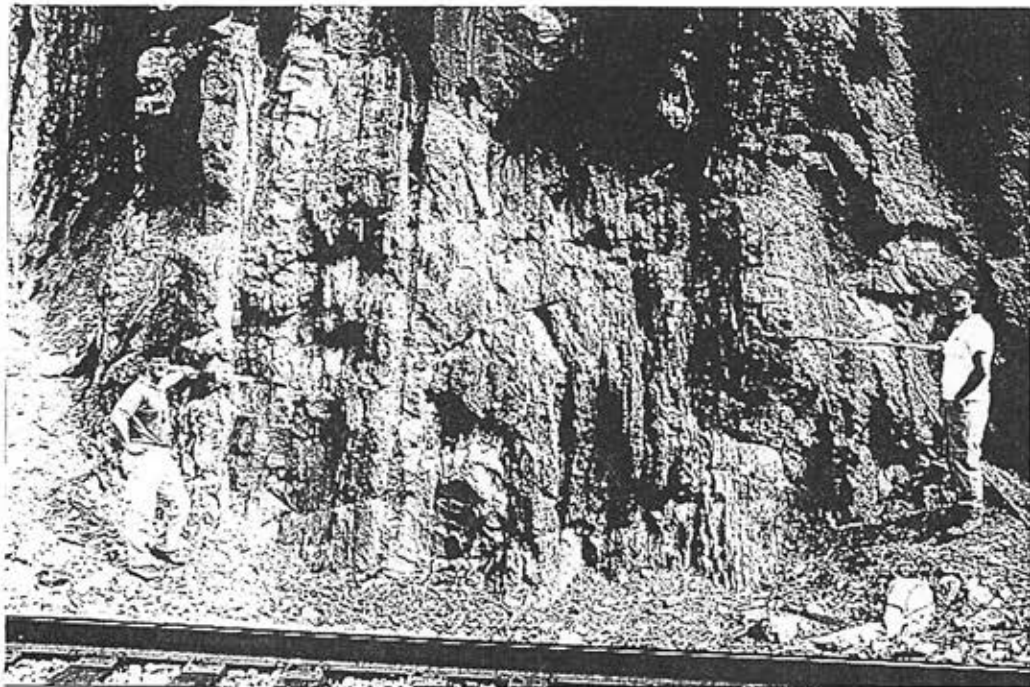
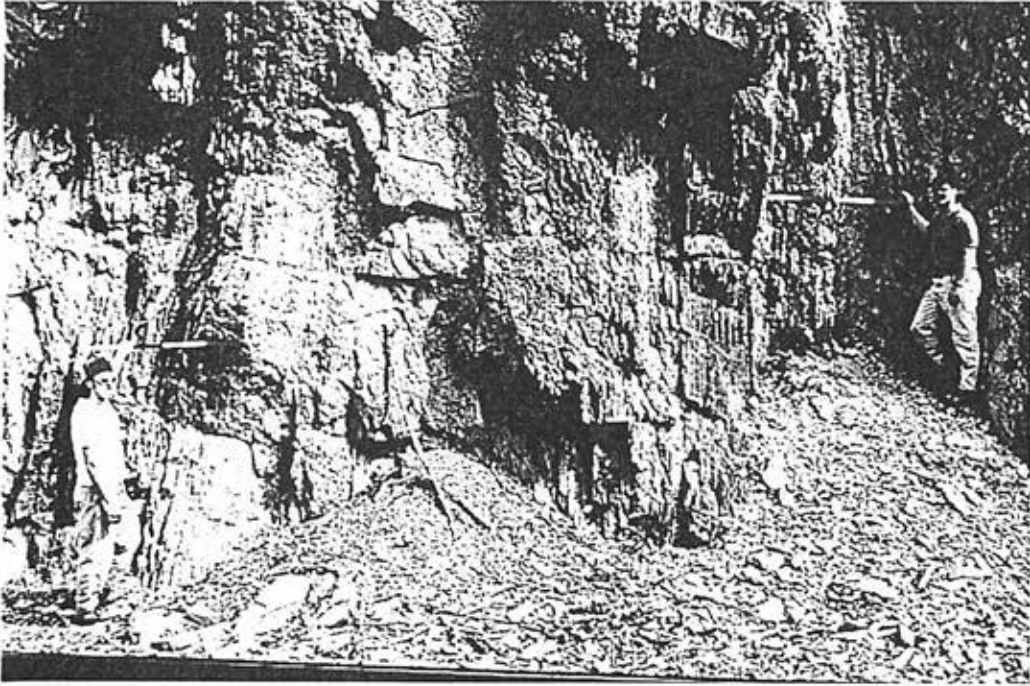


Figure 24. Fifth-order Sequences D and A at Pinto, Maryland. Photograph of fifth-order sequence D (top photograph) and Sequence A of the overlying fourth-order sequence (bottom photograph) Sequence D is the most shale-rich fifth-order sequence in the study interval.

PAC A-4 at both localities indicates a subaerial surface evidently not flooded by the final precessional rise in the eccentricity-modulated cycle. Alternatively, PAC A-5 may be represented at both localities as deposits not differentiated as a separate cycle because the dampened rise did not produce a significant facies change in this subaerial environment. The fact that PAC A-4 is twice as thick as the average PAC in the study interval supports this interpretation.

Sequence B

Fifth-order Sequence B, 14.5 feet thick at Pinto (Figure 24) and 19.0 feet thick at Mt. Union (Figure 25), is divisible into five PACs at Pinto and four at Mt. Union. In general, this sequence is considered more marine than Sequence A because it has a higher carbonate content at both localities. At Pinto, this interval was mined for cement because of its high carbonate content.

Comparatively, Sequence B is carbonate-rich at Pinto and shale-rich at Mt. Union (Figure 26 and 27), where only the first two PACs (B-1 and B-2) contain significant carbonate. The basal PAC (Cycle B-1) at both localities consists of a thick subtidal limestone bed overlain by intertidal cryptalgal laminites. The next three PACs at Pinto (B-2, B-3 and B-4) are basically intertidal carbonate cycles with thin, possibly subtidal bases. In contrast, the same three PACs at Mt. Union consist largely of supratidal shale with very thin intertidal–restricted subtidal basal beds. At Pinto, Sequence B is capped by a shale-rich fifth PAC (B-5) similar to PACs 2, 3, and 4 at Mt. Union. At Mt. Union this PAC is missing owing to hiatus.

Pinto- Sequence B

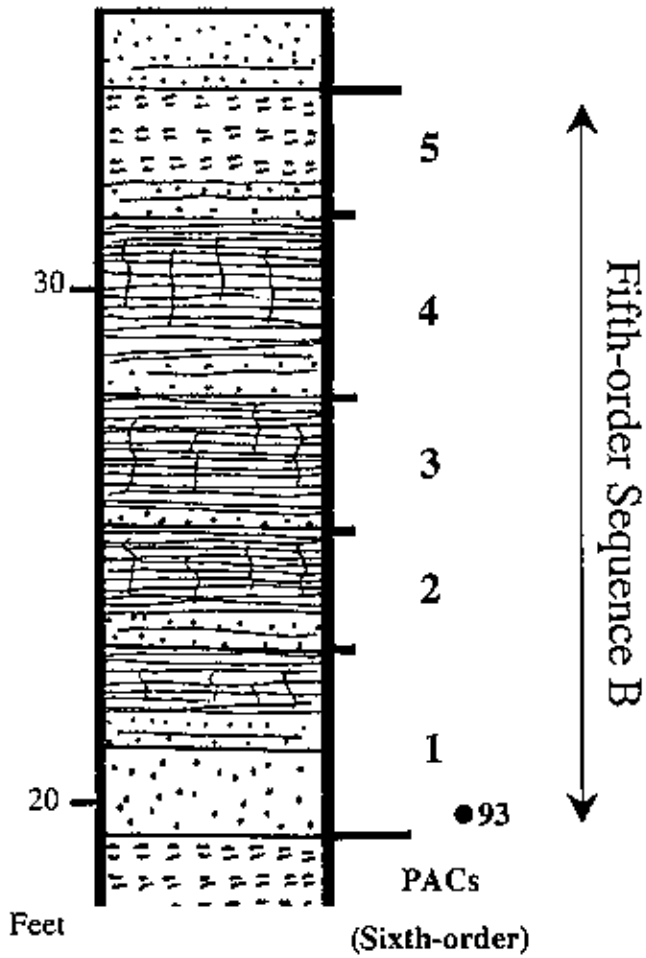


Figure 25. Stratigraphic Column of Sequence B at Pinto. Sequence B is divisible into five PACs, numbered 1 through 5. Numbered black dot indicates a sample location.

Mt. Union- Sequence B

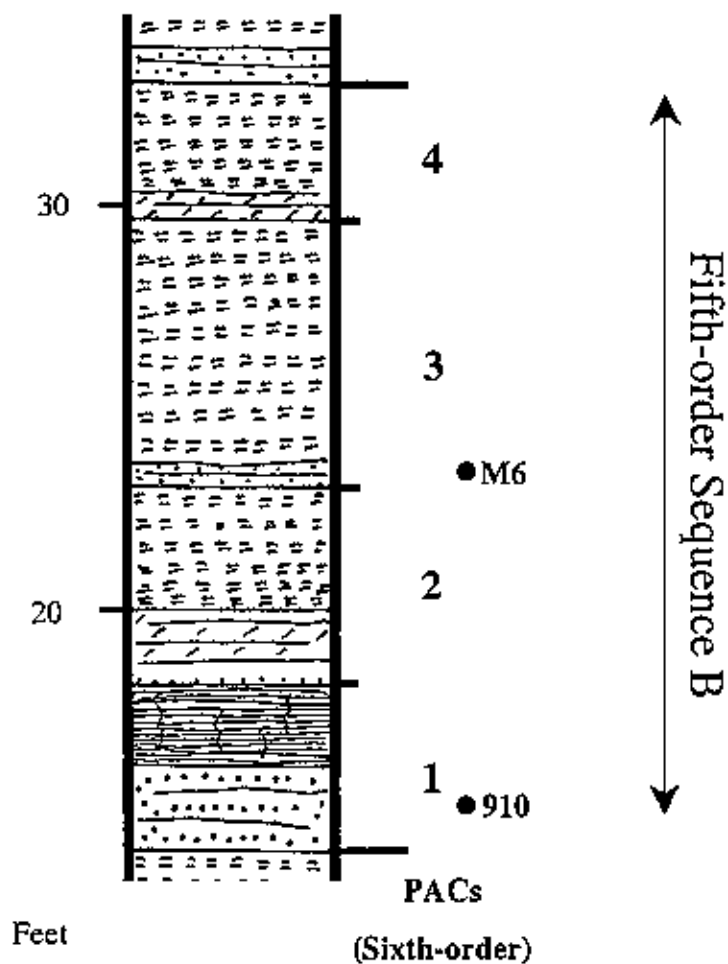


Figure 26. Stratigraphic Column of Sequence B at Mt. Union. Sequence B is divisible into four PACs, numbered 1 through 4. Numbered black dots indicate sample locations.

In summary, Sequence B is more complete and contains more carbonate facies at Pinto, relative to Sequence B at Mt. Union, suggesting deposition in a slightly more offshore position. At both localities Sequence B is the most carbonate-rich sequence in the study interval.

Sequence C

Fifth-order Sequence C, which is 16.0 feet thick at Pinto and 19.5 feet thick at Mt. Union and consists of five PACs at both localities, begins the shallowing trend for the remainder of the studied fourth-order sequence (Figure 30 and 31). For example, at Pinto this sequence contains a greater thickness of supratidal shale than occurs in the prior two sequences (Sequence A and Sequence B). This sequence for the first time at both localities contains supratidal facies in the last two sixth-order sequences, another indication of a shallowing trend in the fourth-order sequence.

The onshore-offshore trend is evident throughout Sequence C (Figure 23, 28 and 29), beginning with PAC C-1 at Pinto (3.5 feet thick) which contains subtidal and intertidal facies, (Figures 9, 10, 11 and 12) in contrast to the intertidal carbonate and supratidal shale in the same PAC at Mt. Union. Similarly, PAC C-3 contains slightly more marine facies at Pinto than at Mt. Union. Finally, the greater thickness of supratidal facies at Mt. Union supports the existence of generally shallower environments at that locality.

Sequence D

Fifth-order Sequence D, 18.0 feet thick at Pinto (Figure 32) and 15 feet thick at Mt. Union, consists of five PACs at Pinto, but only three at Mt. Union (Figure 33).

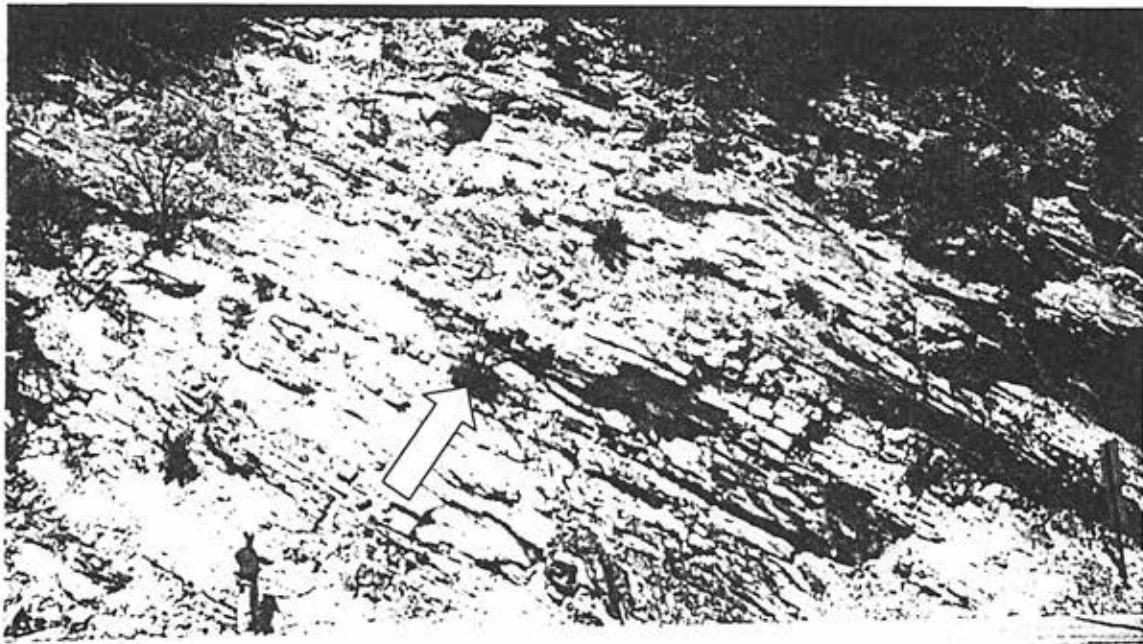
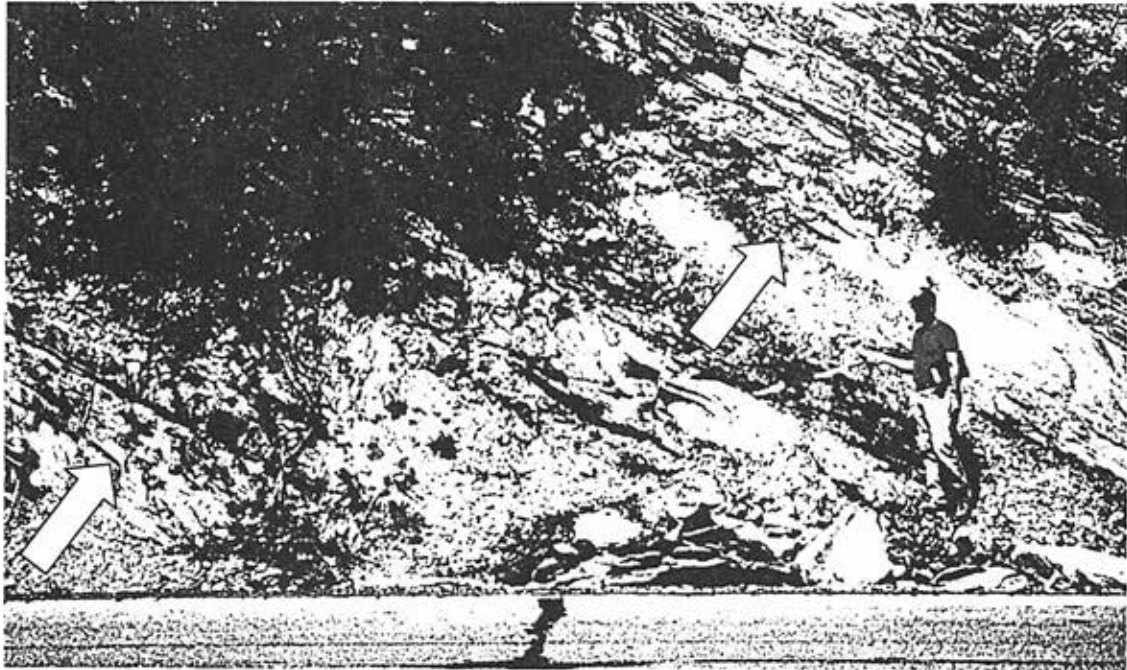


Figure 27. Fifth-order Sequences A and B at Mt. Union, PA . The white arrows point to the base (left arrow) and top (right arrow) of Sequence A in the upper photograph. The geologist points to the A-B sequence boundary in the lower photograph and the white arrow points to the upper boundary of Sequence B. Carbonate beds stand out in relief.

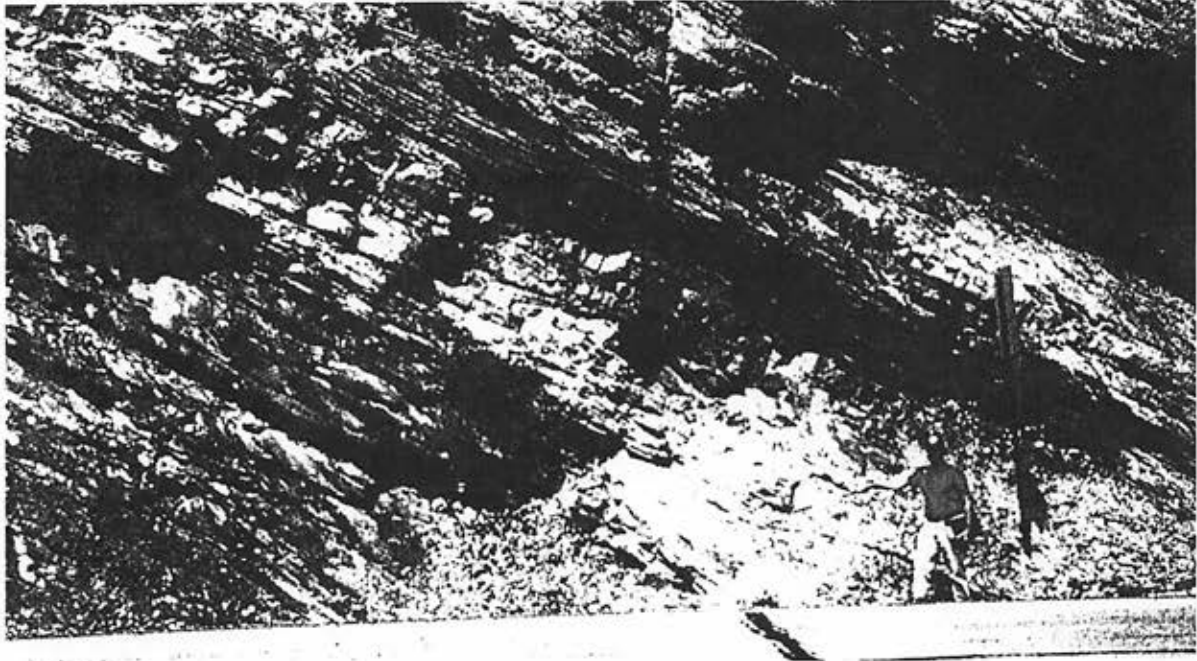


Figure 28. Fifth-order Sequences B and C at Mt Union, PA. Geologist points to the top of Sequence B in the upper photograph. The white arrow points to the B-C sequence boundary in the lower photograph. Carbonate beds stand out in relief.

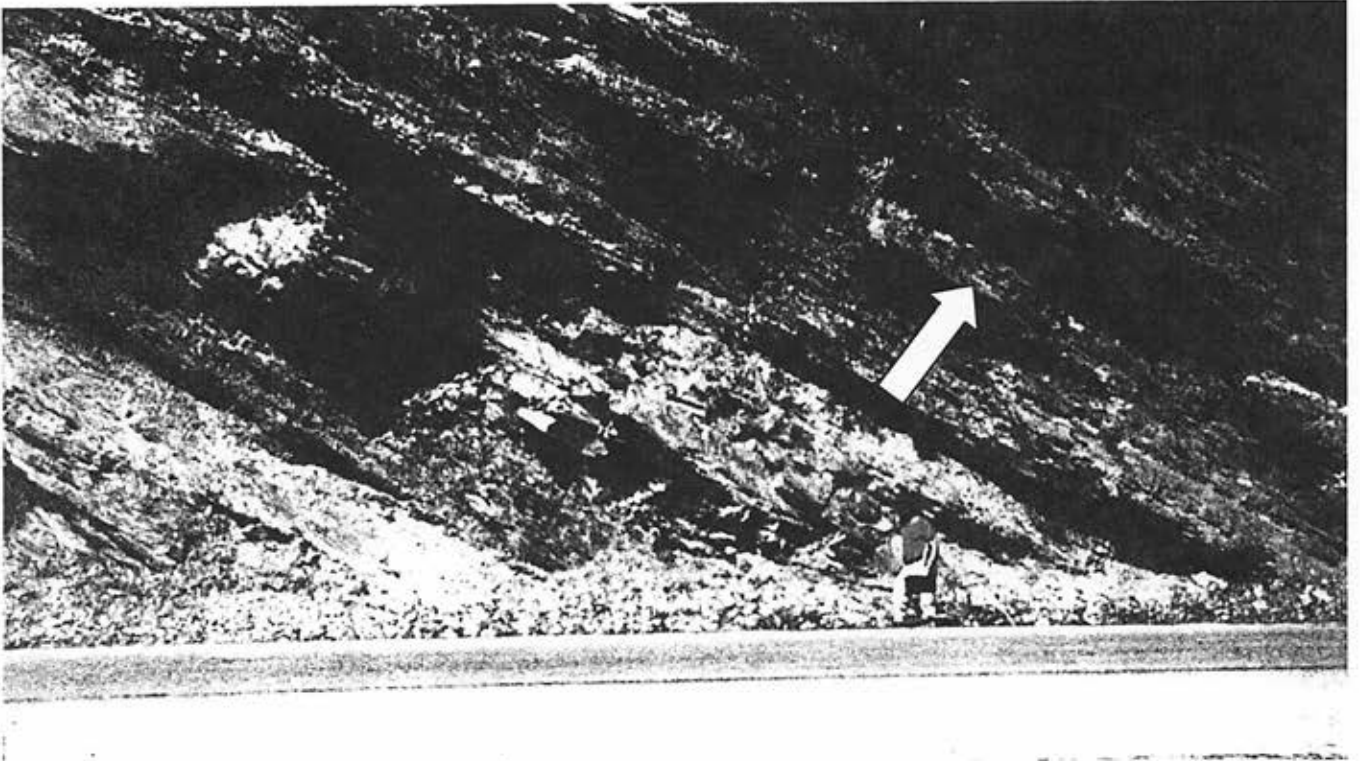


Figure 29. Fifth-order Sequence D at Mt. Union, PA. Geologist points to the top of Sequence C in this photograph and the white arrow points to the top of Sequence D. Sequence D is the most shale-rich fifth-order sequence in the study interval.

Pinto- Sequence C

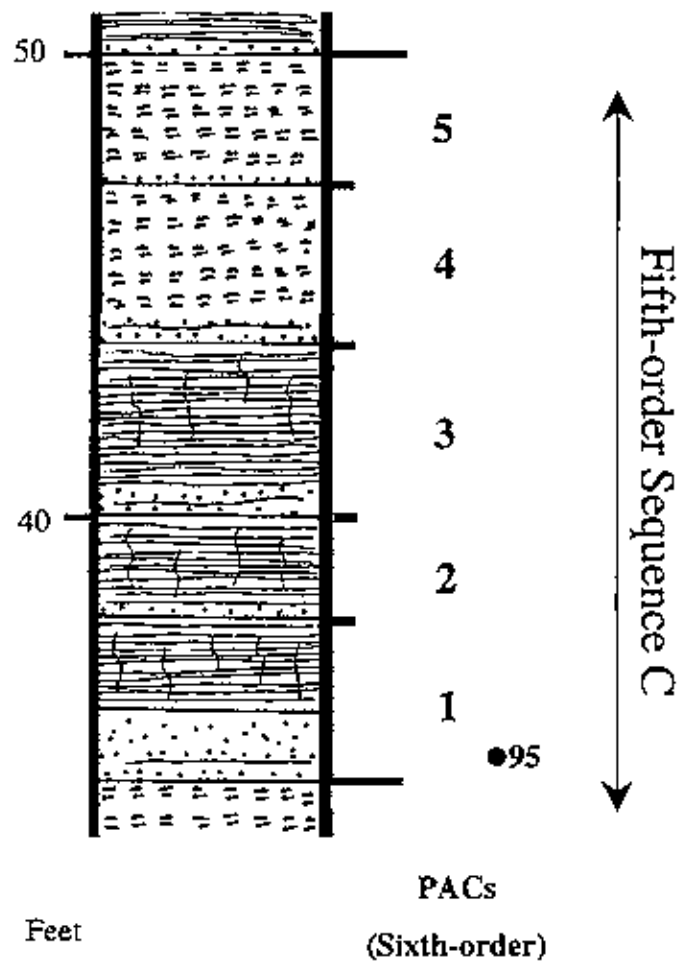


Figure 30. Stratigraphic Column of Sequence C at Pinto. Sequence C is divisible into five PACs, numbered 1 through 5. Numbered black dot indicates a sample location.

Mt. Union- Sequence C

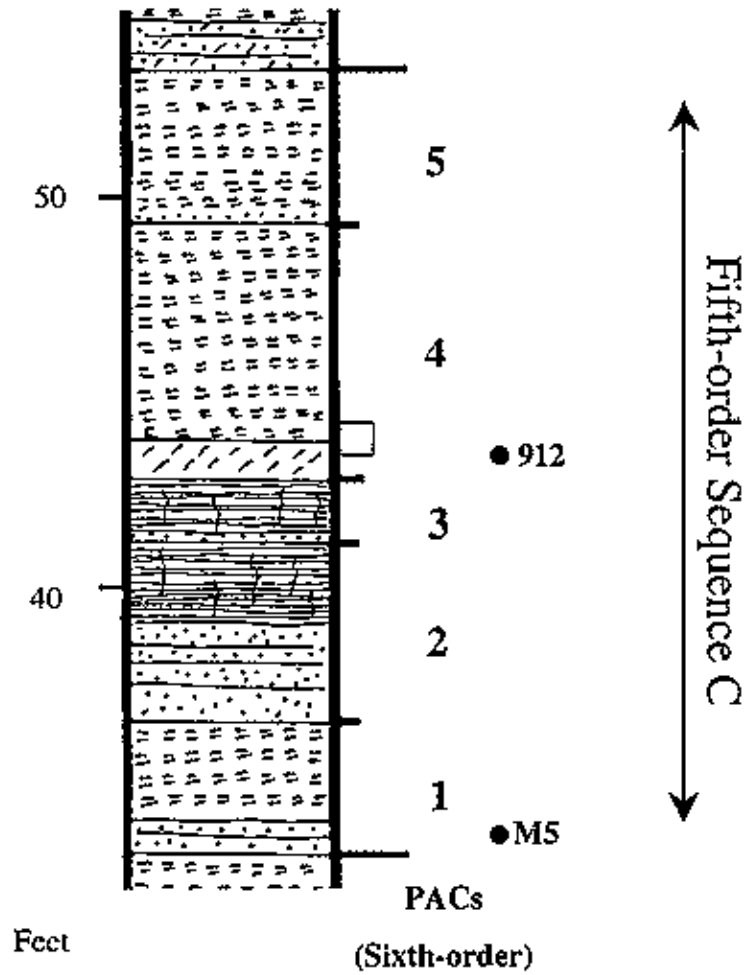


Figure 31. Stratigraphic Column of Sequence C at Mt. Union. Sequence C is divisible into five PACs, numbered 1 through 5. Numbered black dots indicates sample locations.

Internally, Sequence D (Figure 24, 28 and 29) is largely shale-rich at both localities with a slightly higher carbonate content at Pinto owing to the offshore position of that locality. For example, PACs D-1 and D-2 at Pinto consist of subtidal to intertidal facies. In contrast, at Mt. Union PAC D-1 consists of high intertidal to supratidal facies and PAC D-2 consists entirely of high intertidal facies. Additional evidence that Pinto is the more offshore locality includes the presence of supratidal facies in PAC D-3 at Mt. Union in contrast to the intertidal facies at Pinto and the presence of PACs D-4 and D-5 at Pinto in contrast to the absence (by hiatus) at Mt. Union. Overall, Sequence D has the highest shale content of any of the fifth-order sequence investigated in this study. Therefore, it is the most environmentally restricted within the entire fourth-order sequence. Furthermore, Mt. Union contains greater subtidal facies, which further supports the existence of generally shallower facies at that locality.

Conclusion

The vertical pattern of fifth-order sequences within the fourth-order sequence follows a specific stacking pattern as predicted by the PAC model. This pattern begins with Sequence A reversing the shallowing trend of the previous fourth-order sequence. Sequence B is deeper than Sequence A and is the deepest fifth-order sequence within the fourth-order sequence. Sequence C is shallower than sequence B. Sequence D is the shallowest fifth-order sequence within the fourth-order sequence. There is evidence for Pinto having been farther offshore than Mt. Union throughout deposition of the fourth-order sequence.

Pinto- Sequence D

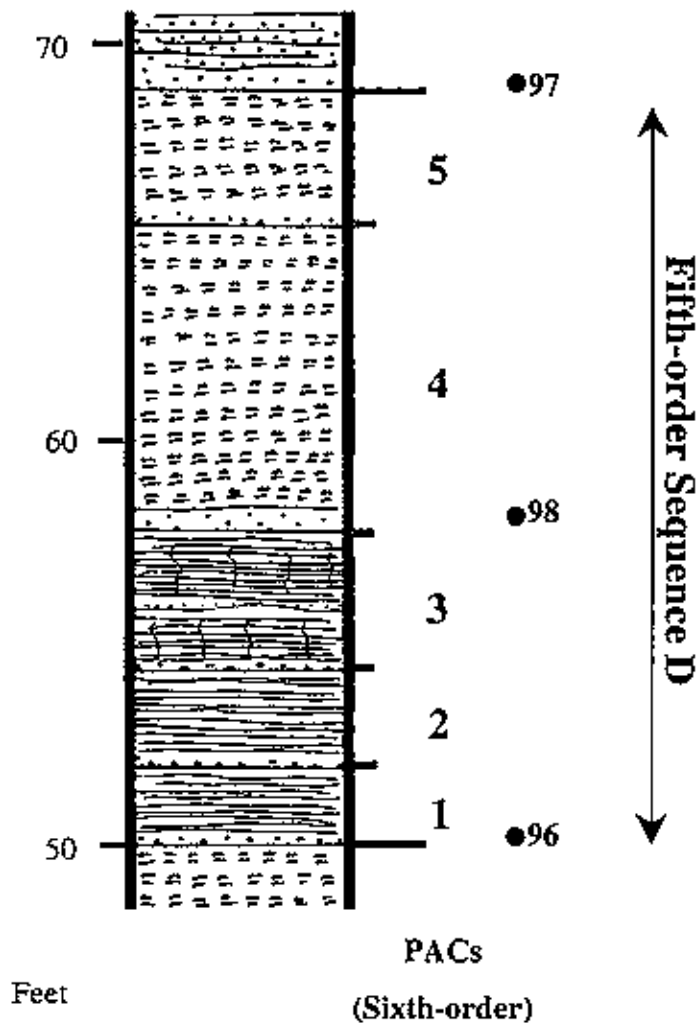


Figure 32. Stratigraphic Column of Sequence D at Pinto. Sequence D is divisible into five PACs, numbered 1 through 5. Numbered black dots indicate sample locations.

Mt. Union- Sequence D

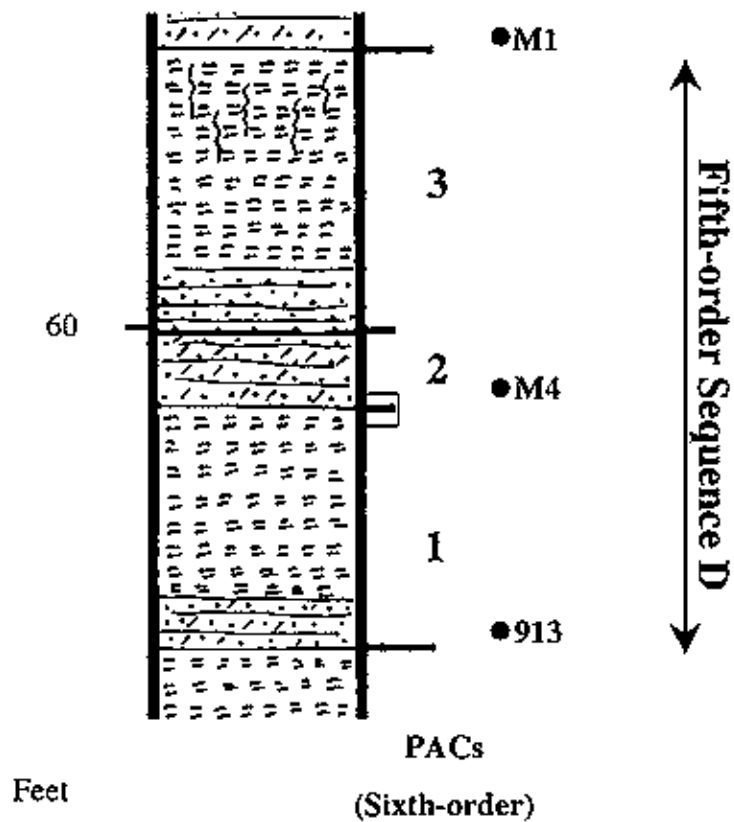


Figure 33. Stratigraphic Column of Sequence D at Mt. Union. Sequence D is divisible into three PACs, numbered 1 through 3. Numbered black dots indicate sample locations.

Evidence includes:

1. greater abundance of subtidal and intertidal carbonates at Pinto;
2. greater supratidal shale content at Mt. Union;
3. greater faunal abundance and diversity at Pinto;
4. more sixth-order cycles missing at Mt. Union.

CHAPTER 5

PALEOENVIRONMENTS, PALEOGEOGRAPHY, BASIN DYNAMICS

Paleoenvironments

Facies analysis throughout the study interval indicates that the whole fourth-order sequence was deposited in peritidal conditions ranging from shallow restricted subtidal to supratidal environments on a gently sloping ramp. Given that all fifth-order sequences within the studied interval terminate in shaley supratidal facies, the general environmental setting appears to be an irregular, muddy, prograding shoreline, bordering restricted subtidal environments. Relatively open, nearly normal marine conditions prevailed immediately following precessional sea-level rises, particularly those enhanced rises marking fifth-order boundaries. As a whole, the fourth-order sequence contains a record of 400 ky of environmental evolution of those near-shore conditions.

Fourth-order sequences in the Wills Creek Formation are characterized by general shallowing following deep or open marine conditions in the second fifth-order sequence as a function of modulation by long eccentricity. The remaining two fifth-order sequences, in the fourth-order sequence, are characterized by episodic deepening events of incrementally lesser magnitude than those defining the second fifth-order sequence. For example, at the end of the fourth-order sequence below the studied interval, Mt. Union and Pinto were dominated by extensive high intertidal to supratidal facies. The first fifth-order sequence in the study interval consists of subtidal calcarenite facies at the base, beginning a trend of more open marine conditions (Figure 31). This trend continues into the second fifth-order sequence, where the most open marine conditions are found at

both localities (Figure 25, 26 and 31). After the most open marine facies, each subsequent fifth-order sequence contains less of the subtidal facies and more intertidal and supratidal facies. For example, fifth-order Sequence C (Figure 30 and 31), at both localities, is dominantly laminated limestone and red/green shale. Sequence D, exemplifying the most restricted facies, contains laminated and massive dolomite at its base and red/green shale at its top.

Fifth-order sequences follow a similar facies pattern between localities, but internally there are significant small-scale environmental fluctuations. These environmental fluctuations detail a sea-level history of shallowing punctuated by deepening events every 20 ky, recorded in sixth-order cycles. For example, open marine conditions caused by amplified precessional sea-level rises characterize the lower portion of each 100 ky sequence, specifically the first two sixth-order sequences. Shallower conditions prevail in the remaining one to three sixth-order cycles as a result of by dampening of the precessional signal by decreasing eccentricity in the short eccentricity cycle (Figure 31). Despite the frequent occurrence of open conditions in the lower section of each fifth-order sequence, supratidal to high intertidal conditions recur at the top each PAC (i.e. every 20 ky). These sixth-order sequences allow for a detailed reconstruction of paleogeography and can be used for accurate interpretation of basin dynamics throughout the entire fourth-order sequence.

Paleogeography

Several studies have investigated the Central Appalachian Foreland Basin paleogeographic setting during the middle to Late Silurian

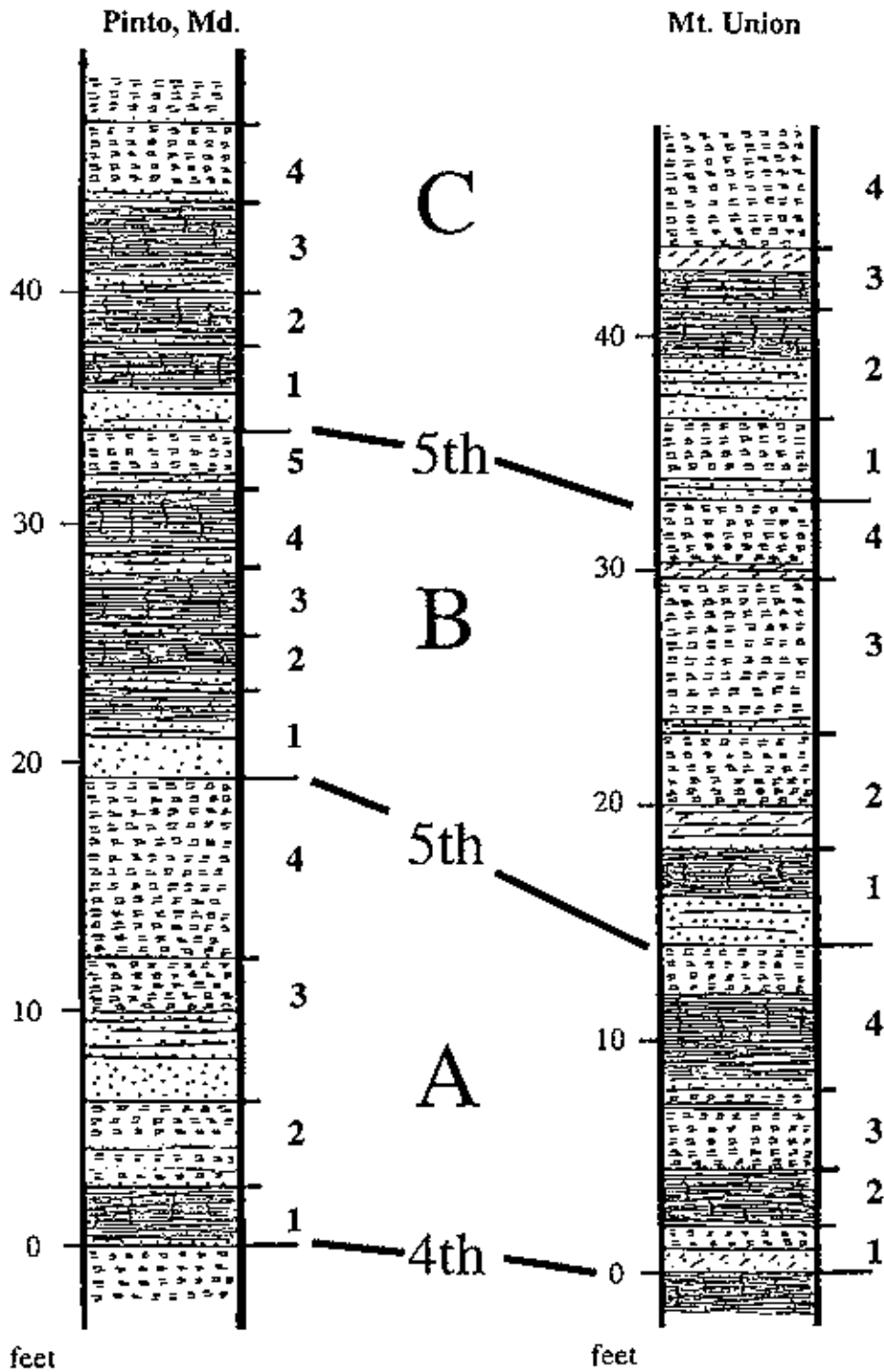
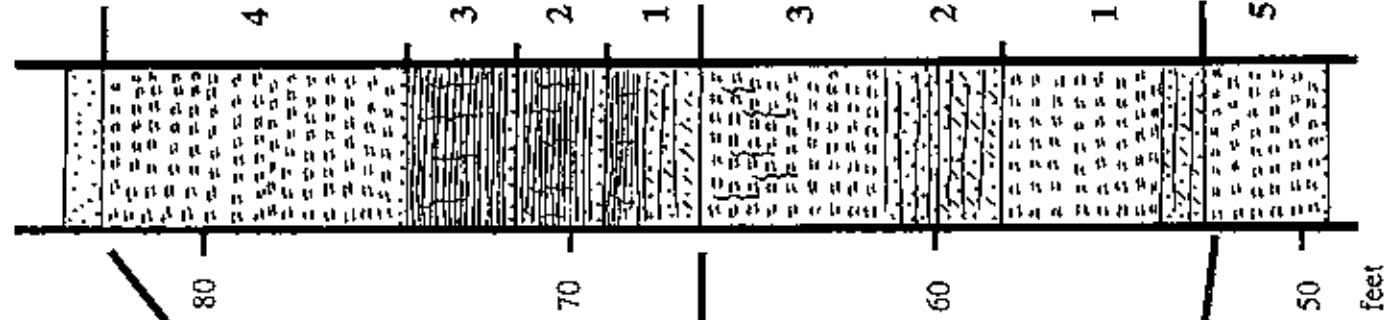


Figure 34. Correlation of Fifth-order Sequences. Patterns of facies change define the fifth-order sequence (A-D). Each fifth-order sequence is divisible into sixth-order sequences (1-5).

Mt. Union, Pa.



5th

A

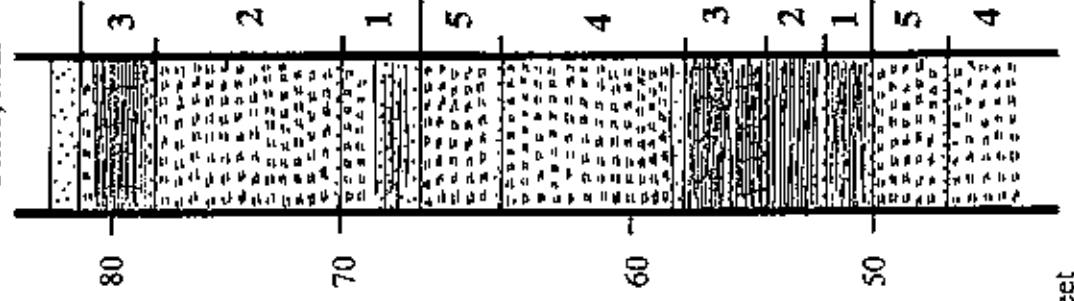
4th

D

5th

C

Pinto, Md.



feet

Figure 34 (continued). Correlation of Fifth-order Sequences. Fifth-order sequences C and D in the upper part of the studied fourth-order sequence and the first fifth-order sequence, Sequence A, of the overlying fourth-order sequence.

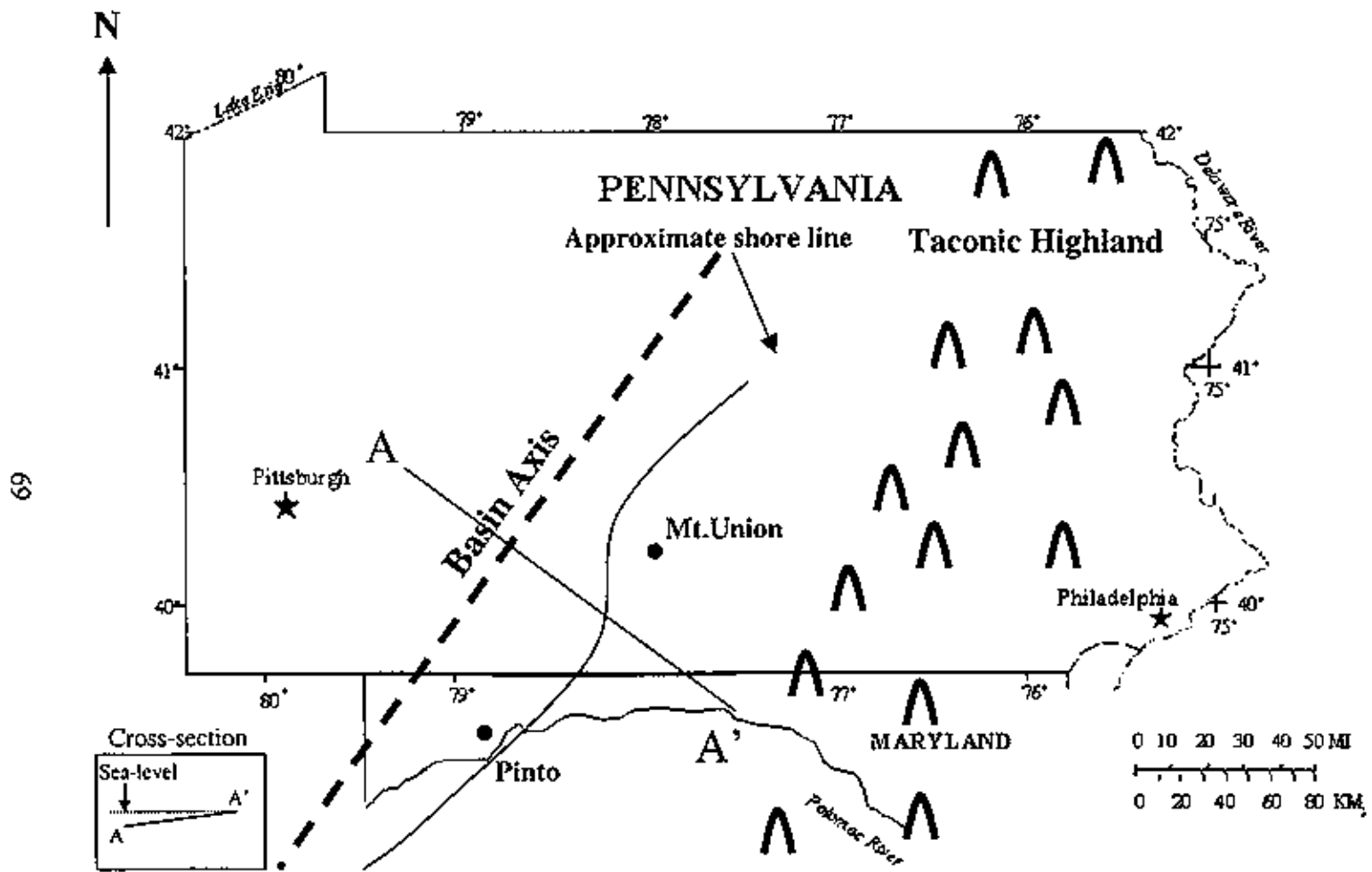


Figure 35. Paleogeographic Reconstruction of the Central Appalachian Basin.

(Alling and Briggs; 1961, Smosna and Patchen, 1978; Cotter and Inners, 1986; Cotter, 1988; and Brett et al, 1990). These studies found that middle to Late Silurian sediment accumulated on a gently sloping ramp that deepened gradually from the southeastern margin of the Appalachian Basin to the central basin axis, located near the present northwestern margin of the Valley and Ridge province (Cotter, 1988). The main input of terrigenous sediment was from the northeast, what is now northern New Jersey (Cotter and Inners, 1986). Overall, the trend of the basin axis is southwest to northeast (Brett et al., 1990).

The Wills Creek Formation was deposited in the central part of the Appalachian Foreland Basin (Figure 35). The basin's southeastern margin is a linear belt of uplifted Middle and Upper Ordovician shales and sandstones. Farther east the Taconic highlands supplied the siliciclastic sediments for the Upper Silurian deposits (Brett et al., 1990).

An onshore-offshore trend between localities is supported by the greater amount of green shale facies (shallowest facies) at Mt. Union (36.5 feet) relative to Pinto (27 feet). A higher faunal content and an overall higher carbonate content give further evidence for environments at Pinto being more marine. This pattern of onshore for Mt. Union and offshore for Pinto is pervasive throughout each fifth-order sequence.

Basin Dynamics

The studied fourth-order sequence is ideal for discriminating the relative roles of tectonism and eustasy in building the Wills Creek Formation. Uniform thickness of the fifth-order sequences and persistence of peritidal conditions are indications of uniform subsidence throughout the time of deposition of the Wills Creek Formation. Therefore,

changes in paleoenvironmental conditions within the basin are solely a function of eustatic sea-level fluctuations. The general subsidence rate for the Salina Supersequence (Tonoloway and Wills Creek Formations), using an average thickness of 358 meters and duration of 10 Ma., is 0.04 m/ky. This value is comparable to values calculated by Osleger and Read (1991) which ranged from 0.06 to 0.25 m/ky for Cambrian sequences.

Given constant subsidence at 0.04 m/ky, the three-tiered hierarchy of cyclic facies patterns in the Wills Creek Formation is a function of a hierarchic allocyclic mechanism. The most likely mechanism is orbital forcing because the stacking patterns of the study interval match predictions of the Milankovitch model. Specifically, the patterns of facies change are consistent with precession as a basic cycle producer which is modulated by eccentricity at two scales: short eccentricity (fifth-order); and long eccentricity (fourth-order).

In conclusion, orbital mechanisms are the most reasonable explanation for the hierarchic cyclic pattern present within the Wills Creek Formation. Matching of observations to the predictions of the model supports this conclusion. Observations include patterns of facies change and cycle thickness throughout the studied interval of the Wills Creek Formation.

The significance of this study is that it documents that orbital forcing was a mechanism operating in the Silurian Period. The study further illustrates that an allocyclic approach can discriminate significant differences in paleoenvironmental and paleogeography at the scale of 20 ky time-slices. Adoption of a process-determined hierarchy of allocycles as a model of stratigraphic analysis may yield similar results in any cyclic sequence.

REFERENCES CITED

- Anderson, E. J., Goodwin, P. W., and Sobieski, T. H., 1984, Episodic accumulation and the origin of formation boundaries in the Helderberg Group of New York State: *Geology*, vol. 12, p. 120-123.
- Anderson, E. J., Goodwin, P. W., and Goodman, P. T., 1986, Reconstruction of patterns of differential subsidence using an episodic stratigraphic model. In Allen, P.A and Homewood, P. eds., Foreland Basins, Special Publication Number 8 of the International Association of Sedimentologists, p. 437-443.
- Balog, A., Haas, J., Read, J. F. and Coruh, C., 1997, Shallow marine record of orbitally forced cyclicity in a Late Triassic carbonate platform, Hungary: *Journal of Sedimentary Research*, vol. 4, no. 4, p. 661-675.
- Bassinot, F. C., Labeyrie, L. D., Vincent, E., Quidelleur, X., Shackleton, N. J. and Lancelot, Y., 1994, The astronomical theory of climate and the ice age of the Brunhes-Matuyama magnetic reversal: *Earth and Planetary Letters*, vol. 126, p. 91-108.
- Berg, T. M., McInerney, M. K., Way, J. H., and MacLachlan, D. B., 1983, Stratigraphic Correlation Chart of Pennsylvania. General Geology Report 75.
- Berger, A., 1988, Milankovitch theory and climate: *Reviews in Geophysics*, vol. 26, p. 624-657.
- Berger, A. and Loutre, M. F., 1992, Astronomical solutions for paleoclimate studies over the last 3 million years: *Earth and Planetary Letters*, vol. 111, p. 369-382.
- Busch, R. M. and Rollins, H. B., 1984, Correlation of Carboniferous strata using a hierarchy of transgressive-regressive units: *Geology*, vol. 12, p. 471-474.
- Chadwick, W. J., 1994, Correlation of Milankovitch-band cyclicity in the peritidal carbonates of the Tonoloway Formation, central Pennsylvania and western Maryland: M. A. Temple University, p. 68.
- Cotter, E., 1988, Hierarchy of sea-level cycles in the medial Silurian siliciclastic succession of Pennsylvania, *Geology*, vol. 16, p. 242-245.
- De Boer, P. L. and Smith, D. G., 1994, Orbital forcing and cyclic sequences: Special Publication of International Association of Sedimentologists, vol. 19, p. 1-14.

- Elrick, M., 1996, Sequence stratigraphy and platform evolution of Lower-Middle Devonian carbonates, eastern Great Basin: *Geological Society of America Bulletin*, vol. 108, no. 4, p. 392-416.
- Fischer, A. G. and Bottjer, D. J., 1991: Orbital forcing and sedimentary sequences: *Journal of Sedimentary Petrology*, vol. 7, p. 1063-1069.
- Goldhammer, R. K., Dunn, P. A., and Hardie, L. A., 1990, Depositional cycles, composite sea-level changes, cycle stacking patterns, and the hierarchy of stratigraphic forcing: examples from Alpine Triassic platform carbonates: *Geological Society of America Bulletin*, vol. 102, p. 535-562.
- Goldhammer, R. K. and Oswald, E. J., 1994, High-frequency, glacio-eustatic cyclicity in the Middle Pennsylvanian of Paradox Basin: an evaluation of Milankovitch forcing: *Special Publication of International Association of Sedimentologists* vol. 19, p. 243-283.
- Goodman, W. M., and Brett, C. E., 1994, Roles of eustacy and tectonics in development of Silurian stratigraphic architecture of the Appalachian Foreland Basin: Tectonic and Eustatic Controls on Sedimentary Cycles, *SEPM Concepts in Sedimentology and Paleontology* vol. 4 , p. 147-169.
- Goodwin, P. W., and Anderson, E. J., 1985, Punctuated aggradational cycles: a general hypothesis of episodic stratigraphic accumulation: *Journal of Geology*, vol. 93, p. 515- 533.
- Goodwin, P. W., Anderson, E. J., Goodman, W. M. and Saraka, L. J., 1986, Punctuated aggradational cycles: implications for stratigraphic analysis. In: M. A. Arthur and G.E. Garrison eds., Devonian of the World, Volume II: Sedimentation, *Canadian Society of Petroleum Geologists*, p. 553-568.
- Goodwin, P. W. and Anderson, E. J., 1988, Episodic development of the Helderbergian paleogeography New York State Appalachian Basin: in McMillian, N.J., Embry, A.F. and Glass, D.J., eds. Milankovitch Cycles through Time. *Paleoceanography*, vol. 1, p. 417-429.
- Goodwin, P. W. and Anderson, E. J., 1997, Stratigraphic Incompleteness: Milankovitch in the Manlius at the Margin: *Guidebook for the 69th Annual Meeting*, New York State Geological Assoc., p. 237-249.
- Hoskins, D. M., 1961, Stratigraphy and palcontology of the Bloomsburg Formation of Pennsylvania and adjacent states: *Pennsylvania Topographic and Geological Survey Bulletin*, vol. G36, p. 48-52 and 61.

- Strasser, A., 1994, Milankovitch cyclicity and high-resolution sequence stratigraphy in lagoonal-peritidal carbonates (Upper Tithonian-Lower Berriasian, French Jura Mountains): Special Publications of the International Association of Sedimentologists: vol. 19, p. 285-301.
- Swartz, C. K., 1923, Geologic relations and geographic distribution of the Silurian strata of Maryland: Maryland Geological Survey, Silurian Volume, p. 40-211.
- Swartz, F. M., 1934, Silurian section near Mount Union, Central Pennsylvania: Bulletin of the Geological Society of America, vol. 45, p. 81-134.
- Swartz, F. M., 1955, Stratigraphy and structure of the Ridge and Valley area from University Park to Tyrone, Mount Union and Lewistown, Pennsylvania. Trip Itinerary: Guidebook of the 21st Annual Field Conference of Pennsylvania Geologists. p. S-1- S-36.
- Vail, P. R., Mitchum, R. M., and Thompson, S. III, 1977, Seismic stratigraphy and global change of sea-level, Part 3: relative changes of sea-level from coastal onlap: In Payton, C.E. ed., Seismic Stratigraphy- Applications to Hydrocarbon Exploration: American Association of Petroleum Geologists Memoir, vol. 26, p. 63-81.
- Zeliznak, C., Brown, S. M., Goodwin, P. W and Anderson, E. J., 1997, Facies patterns that define Wills Creek 5th and 6th order cycles: Abstracts with Programs, Geol. Soc. Amer. Northeastern Section, vol. 29, no. 1, p. 92.


APPENDIX A

COMPLETE COLUMNAR SECTION, PINTO, MARYLAND

**Complete Columnar Section, Pinto, Maryland. Comparison of Swartz (1923)
lithologic description with the column used in this study.**

Studies Thickness	Current Column	Cycle boundaries	Swartz (1923) Thickness of Beds		Swartz (1923) Total Thickness of formation		Swartz (1923) Lithologic Description
			Ft.	In.	Ft.	In.	
30 20 10 0		C	1	7	181	9	Dark, compact limestone.
			2	0	180	2	Calcareous mud rock, breaks irregularly and weathers green.
			0	10	178	2	Calcareous shale.
		B	2	3	177	4	Dark fissile calcareous shale, surfaces covered with mud cracks
			4	0	175	1	Laminated, argillaceous limestone with interbedded shale
			4	8	171	1	Fissile black calcareous shale covered with mud cracks
		A	1	6	166	5	Hard, dark-brown limestone
			4	8	164	11	Fissile black calcareous shale covered with mud cracks
			3	0	156	3	Bedded limestone
			2	4	153	3	Fissile black calcareous shale with a few thin layers of laminated limestone
4th	1	1	149	11	Laminated argillaceous limestone stained yellow		
	1	11	146	10	Mudrock, breaking irregularly, weathers greenish		

Complete Columnar Section, Pinto, Maryland. (continued)

Thickness of 4 th order cycle	Current Column	Cycle boundaries	Swartz (1923) Thickness of Beds	Swartz (1923) Total Thickness of formation	Swartz (1923) Lithologic Description		
Ft.		5th	1 11	227 11	Thick-bedded, argillaceous limestone, weathers yellowish.		
			1 4	226 0	Mud rock, weathers greenish		
			1 9	224 8	Laminated argillaceous limestone.		
			3				
			A	2	7 1	222 11	Calcareous mud rock.
				1	1 4	215 10	Argillaceous limestone.
				4th	1 8	214 6	Banded argillaceous limestone weathers yellow
					5		
				D	4	9 2	212 10
			3		1 8	203 8	Laminated calcareous shale
2	2 4	202 0	Thin-bedded, argillaceous limestone				
1	3 9	199 8	Thin-bedded, argillaceous limestone with some calcareous shale				
5th	5	6 6	195 11		Calcareous mud rock, upper part weathers green		
	4						
	C	3	7 8	189 5	Dark, fissile, calcareous shale with some argillaceous limestone bands		
		2					
		1	1 7	181 9	Dark, compact limestone		